The EMBO Journal (2007) 26, 1749–1760 | © 2007 European Molecular Biology Organization | All Rights Reserved 0261-4189/07
www.embojournal.org

THE EMBO JOURNAL

Reactive oxygen species are essential for autophagy and specifically regulate the activity of Atg4

Ruth Scherz-Shouval, Elena Shvets, Ephraim Fass, Hagai Shorer, Lidor Gil and Zvulun Elazar*

Department of Biological Chemistry, The Weizmann Institute of Science, Rehovot, Israel

Autophagy is a major catabolic pathway by which eukaryotic cells degrade and recycle macromolecules and organelles. This pathway is activated under environmental stress conditions, during development and in various pathological situations. In this study, we describe the role of reactive oxygen species (ROS) as signaling molecules in starvation-induced autophagy. We show that starvation stimulates formation of ROS, specifically H_2O_2. These oxidative conditions are essential for autophagy, as treatment with antioxidative agents abolished the formation of autophagosomes and the consequent degradation of proteins. Furthermore, we identify the cysteine protease HsAtg4 as a direct target for oxidation by H_2O_2, and specify a cysteine residue located near the HsAtg4 catalytic site as a critical for this regulation. Expression of this regulatory mutant prevented the formation of autophagosomes in cells, thus providing a molecular mechanism for redox regulation of the autophagic process.

The EMBO Journal (2007) **26,** 1749–1760. doi:10.1038/sj.emboj.7601623; Published online 8 March 2007
Subject Categories: membranes & transport
Keywords: Atg4; autophagy; GATE-16; ROS

Introduction

Autophagy is a major pathway for delivery of proteins and organelles to lysosomes/the vacuole, where they are degraded and recycled. Autophagy plays an essential role in differentiation and development, as well as in cellular response to stress. It is activated during amino-acid deprivation and has been associated with neurodegenerative diseases, cancer, pathogen infections and myopathies (reviewed in Cuervo, 2004; Shintani and Klionsky, 2004). Autophagy is initiated by the surrounding of cytoplasmic constituents by the crescent-shaped isolation membrane/phagophore, which forms a closed double-membrane structure, called autophagosome. Finally, the autophagosome fuses with a lysosome to become an autolysosome, and its content is degraded by lysosomal hydrolases.

*Corresponding author. Department of Biological Chemistry, The Weizmann Institute of Science, Rehovot, 76100 Israel.
Tel.: +972 8 9343682; Fax: +972 8 9344112;
E-mail: bmzevi@wicc.weizmann.ac.il

Received: 31 August 2006; accepted: 24 January 2007; published online: 8 March 2007

The molecular mechanism underlying autophagy has been extensively researched in the past decade, and the genes participating in this process, denoted ATGs (autophagy-related; Klionsky *et al*, 2003), were found to be conserved from yeast to man (Ohsumi, 2001; Huang and Klionsky, 2002). Yet, the roles played by the different gene products and their modes of action are to be resolved. A hallmark event in the autophagic process is the reversible conjugation of the Atg8 family of proteins to the autophagosomal membrane (Ichimura *et al*, 2000). This ubiquitin-like (UBL) protein family, which has been implicated in a variety of cellular processes, includes Atg8p in yeast (Lang *et al*, 1998; Ichimura *et al*, 2000) and GATE-16 (Golgi-associated ATPase enhancer of 16 kDa; Sagiv *et al*, 2000), LC3 (light-chain 3; Mann and Hammarback, 1994) and GABARAP (GABA receptor-associated protein; Wang *et al*, 1999) in mammals. All Atg8 homologues (hereafter termed Atg8s) serve as substrates for the Atg4 family of cysteine proteases (Kirisako *et al*, 2000; Hemelaar *et al*, 2003; Marino *et al*, 2003; Scherz-Shouval *et al*, 2003). Atg4s cleave Atg8s near the C-terminus, downstream of a conserved glycine. This cleavage allows the conjugation of Atg8 to phosphatidylethanolamine (PE) through the exposed glycine, a process mediated through a ubiquitination-like mechanism. Atg8-PE serves as another substrate for Atg4, which cleaves Atg8 and releases it from the membrane. Notably, this conjugation process must be preceded by another ubiquitination-like process, conjugating Atg12 to Atg5 (Tanida *et al*, 2004b). In mammalian cells, amino-acid deprivation induces lipidation of LC3 (Kabeya *et al*, 2000) as well as of GATE-16 and GABARAP (Kabeya *et al*, 2004). Lipidated Atg8s associate with phagophaores and autophagosomes and remain there until fusion with lysosomes, at which point intra-autophagosomal Atg8 is probably degraded (Kabeya *et al*, 2000, 2004).

At least four Atg4 mammalian homologues have been reported based on sequence homology to the yeast *Saccharomyces cerevisiae* (Sc)Atg4. Two of the homologues, HsAtg4A and HsAtg4B, were shown to cleave the three mammalian Atg8s with different efficiencies: HsAtg4A cleaves mainly GATE-16, whereas HsAtg4B cleaves all three homologues (GATE-16, GABARAP and LC3), with the highest efficiency for LC3 (Kabeya *et al*, 2004).

Atg4s act both as conjugating and deconjugating enzymes and therefore their activity is expected to be tightly regulated. Hence, in the process of autophagy, following the initial cleavage of Atg8-like proteins, Atg4 must become inactive so as to ensure the conjugation of Atg8 to the autophagosomal membrane. Later on, as the autophagosome fuses with the lysosome, Atg4 might be locally re-activated in order to delipidate and recycle Atg8. How is this regulation achieved? We have previously shown that recombinant HsAtg4A is active as a cysteine protease of GATE-16 only in the presence of the reducing agent DTT (Scherz-Shouval *et al*, 2003). This

could implicate that, *in vivo*, the delipidating activity of Atg4 is regulated through changes in redox potentials that take place under different conditions and at specific subcellular microenvironments. Such regulation could be inflicted, among other factors, by reactive oxygen species (ROS). At high levels, ROS are deleterious to cells, leading to programmed cell death (PCD) (Jabs, 1999; Lee *et al*, 2003; Macip *et al*, 2003). At low levels, however, ROS can serve as signaling molecules, by oxidizing factors in a variety of pathways that lead to growth and survival. Here, we report for the first time the involvement of ROS as signaling molecules in nutrient starvation-induced autophagy, which is essentially a survival pathway. We show that under starvation conditions, cells form ROS, specifically H_2O_2, which is essential for autophagosome formation and autophagic degradation. The oxidative signal is partially PI3K dependent and leads to inhibition of Atg4. Using an *in vitro* assay, we could demonstrate that H_2O_2 directly regulates HsAtg4A. Moreover, we identified Cys^{81}, situated four amino acids downstream of the active site, as an essential residue for the redox regulation of HsAtg4A. Expression of HsAtg4A mutated in Cys^{81}, or the corresponding mutant of HsAtg4B, inhibited the formation of GATE-16- or LC3-labeled autophagosomes in cells.

Results

Starvation induces formation of ROS

ROS serve as signaling molecules in a variety of cellular processes, including growth, differentiation, adhesion and PCD. To test whether ROS play a role in autophagy, we measured ROS production under starvation using a fluorescent probe, dihydroethidum (DHE). DHE reacts with peroxides to form a compound that upon binding to DNA fluoresces and can be visualized by confocal fluorescent microscopy (Vanden Hoek *et al*, 1997). Indeed, upon nutrient starvation, DHE staining was evident, indicating that cells accumulate peroxides under these conditions (Figure 1A). We then used another probe, 2′,7′-dichlorofluorescin diacetate (DCF-DA), which reacts mainly with H_2O_2 to form a fluorescent compound at the point of interaction (Cathcart *et al*, 1983; Vanden Hoek *et al*, 1997). DCF staining was already evident 15 min after the induction of starvation (Figure 1Bd and Supplementary Figure 1A, see text below). The pattern of DCF staining was punctated as well as cytosolic, and it was also apparent following overnight starvation (Figure 1Bh). These results indicate that H_2O_2 is most likely the oxidative agent accumulating in starved cells. To rule out the possibility that the oxidative signal associated with starvation is leading to PCD, we tested the viability of cells grown under nutrient starvation conditions. As shown in Supplementary Figure 1B, 5 h of nutrient starvation did not affect the viability of the cells, and the percent of cell death was equally low in control and starved cells. Taken together with the finding that the oxidative signal appears minutes after induction of starvation, these results suggest that H_2O_2 serves as a signaling molecule in the autophagic pathway, and not as part of an oxidative stress leading to PCD.

The pattern of DCF staining resembled mitochondrial staining, and therefore we double stained the cells with DCF and MitoTracker Red, a marker for functional mitochondria. We found significant overlap between the two markers (Figure 1Bf and j; enlargements in g and k, respectively). All the DCF puncta either colocalized with or were in close vicinity to MitoTracker-stained structures, suggesting mitochondria as the source of ROS generated during starvation. This finding coincides with our observation that phagophores, identified by a double staining with Atg5 and Atg16 (Mizushima *et al*, 2003), tend to colocalize with MitoTracker Red-stained mitochondria (Supplementary Figure 1C), suggesting a functional link between ROS generated in the mitochondria during starvation and autophagosome formation. This result is consistent with recently reported findings (Kissova *et al*, 2006).

In order to assess the rise in ROS in a more accurate manner, we measured the increase in DCF fluorescence using a fluorimeter set at 485 nm excitation and 535 nm emission in two different cell lines (CHO and HeLa). The cells were either deprived of serum, completely starved (deprived of serum and nutrients) or grown in control medium for 2 h, after which they were treated with DCF and the fluorescent signal of the whole population (3×10^4 cells) was monitored. As shown in Figure 1C, complete starvation of the cells resulted in a dramatic increase in the fluorescent signal over time, as compared to the control, whereas serum starvation had only a mild effect on the fluorescent signal, indicating a slight increase in ROS production. These measurements were further processed and summarized as the increase in DCF fluorescence over 20 min of incubation with the reagent (Figure 1D).

Class III PI3K is involved in starvation-dependent ROS formation

In the attempt to understand where ROS production fits in the autophagic signaling pathway, we monitored the effect of two known autophagy inhibitors, wortmannin and 3-methyladenine (3MA), on starvation-dependent DCF staining (Petiot *et al*, 2000). Starvation of cells for a 2-h period in the presence of either drug reduced the level of DCF fluoresence by 25–30% (Figure 2A, left panel). As expected, the autophagic activity in the treated cells, tested by the rate of degradation of long-lived proteins (known to increase during autophagy, see Mizushima *et al*, 2001), was significantly reduced (Figure 2A, right panel). Wortmannin and 3MA are phosphatidyl inositol 3 kinase (PI3K) inhibitors. Class III PI3K plays a critical role in the early stages of autophagosome formation in mammals through formation of an essential complex with Beclin 1 and, hence, inhibition of its activity inhibits the autophagic process (Petiot *et al*, 2000; Tassa *et al*, 2003). This finding, therefore, indicates that ROS production is partially PI3K dependent. Indeed, partial silencing of Beclin 1 (previously shown to cause a partial autophagic defect; Reef *et al*, 2006) or the PI3K hVps34 resulted in 15 and 20% (respectively) reduction in starvation-induced ROS production (Supplementary Figure 2A). Notably, partial silencing of hVps34 caused 30% reduction in the number of autophagosomes per cell (Supplementary Figure 2B, lower right panel).

Next, we assessed the level of DCF staining in cell lines deleted for the Atg5 gene, whose product is essential for autophagosome formation, acting downstream of the class III PI3K (Suzuki *et al*, 2001; Tanida *et al*, 2004b). DCF staining in the mutant cells did not decrease, as compared with control cells (Figure 2B), but rather increased significantly (40–50%), indicating that ROS production takes place upstream of the

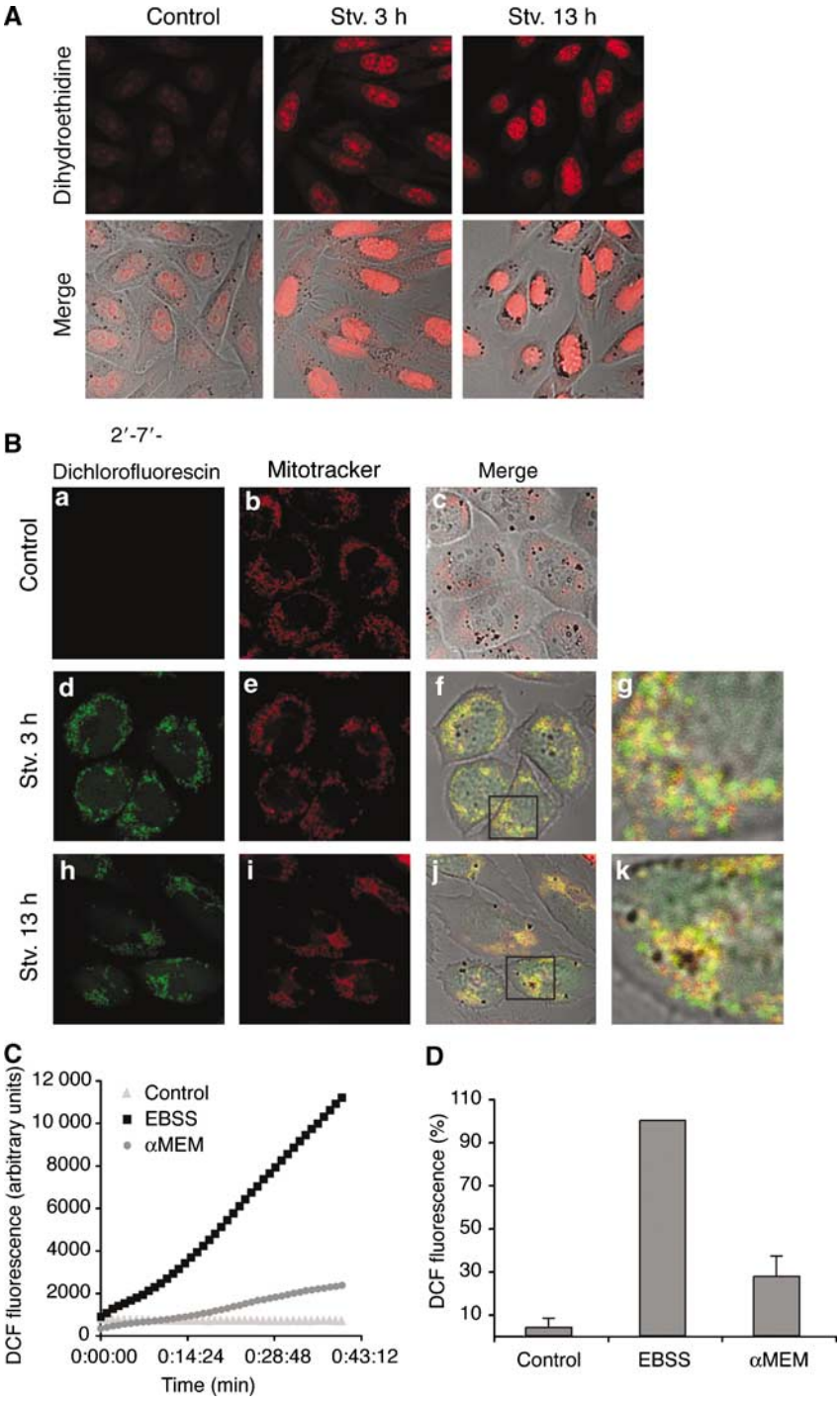

Figure 1 Cells accumulate ROS under starvation conditions. (**A**) CHO cells were grown in a control medium (see Materials and methods) or starved for 3 or 13 h, after which they were incubated in 50 μM DHE and visualized as detailed in Materials and methods. (**B**) CHO cells were grown as in (A), treated with 5 nM MitoTracker Red for 30 min at 37°C, washed, treated with 30 μM DCFDA and visualized as detailed in Materials and methods. (**C**) HeLa cells grown in 96-well plates were deprived of serum (αMEM), completely starved (EBSS) or maintained in a control medium (α-MEM, 10% FCS) for 2 h, after which they were treated with DCFDA as in (B) and subsequently analyzed in a fluorimeter, as explained in Materials and methods. (**D**) Data collected from the fluorometric measurements were analyzed as detailed in Materials and methods.

Atg5-dependent step of autophagosome formation, and suggesting that in the absence of a functional autophagic pathway, cells accumulate ROS.

ROS formation is essential for autophagy

The results described above suggest that starvation induces ROS formation. But are ROS essential for autophagy? To address this question, we tested the effect of *N*-acetyl-L-cysteine (NAC), a general antioxidant, and catalase, which specifically decomposes H_2O_2, on the formation of autophagosomes using GATE-16 and LC3 as markers. LC3 and GATE-16 were shown to label autophagosomes under starvation conditions (Kabeya *et al*, 2004; Supplementary Figure 3A), and as shown in Supplementary Figure 3B, the two proteins

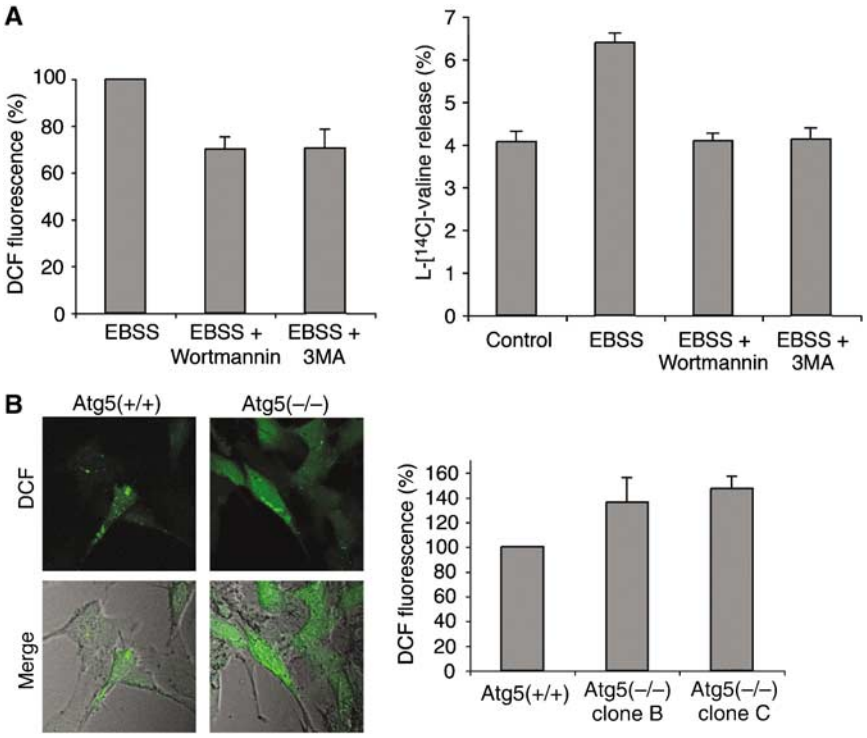

Figure 2 ROS formation occurs partially downstream of class III PI3K activation. (**A**) Left panel: HeLa cells were starved for 2 h in the presence or absence of either 100 nM wortmannin or 10 mM 3MA, after which they were treated with DCFDA and analyzed by a fluorimeter as described above. Right panel: the rate of degradation of long-lived proteins was measured in cells incubated in either α-MEM medium or EBSS medium in the absence or presence of 100 nM wortmannin or 10 mM 3MA. Values are represented as the means ± s.d. of three separate determinations. (**B**) WT MEFs or Atg5 (−/−) MEFs from two separate clones were starved for 2 h before treatment with DCFDA and visualization or fluorometric analysis.

exhibit significant colocalization under these conditions. Addition of either NAC or catalase to the growth medium (Sakurai and Cederbaum, 1998; Preston *et al*, 2001; Xu *et al*, 2003) of the cells for 10 min before a 2-h starvation period resulted in reduced lipidation of GATE-16 and LC3 and abolished the formation of GATE-16- and LC3-labeled autophagosomes (Figure 3A and Supplementary Figure 3C). As expected, the same concentration of antioxidative reagents significantly reduced the level of ROS in the treated cells (Figure 3B). These results were further validated by testing the effect of antioxidants on starvation-induced protein degradation (Figure 3C). Treatment with NAC caused 60% inhibition in starvation-induced degradation, and catalase caused 25% inhibition in starvation-induced degradation. Taken together, we conclude that starvation conditions induce formation of ROS, which are required for induction of autophagy. Notably, treatment of cells with H_2O_2 alone did not result in formation of autophagosomes (data not shown).

Atg4 is attenuated in response to starvation in a redox-dependent manner

Next, we searched for a cellular target of the starvation-induced oxidative signal. The amount of the lipidated form of Atg8s increases significantly during starvation (Kabeya *et al*, 2004). As shown in Figure 4A, this elevation, in mammalian Atg8s, does not result from increased transcription, as previously shown for ScAtg8 (Kirisako *et al*, 1999). Consistently, we could not observe changes in the protein levels of mammalian Atg8s under these conditions (Figure 4B and data not shown). We therefore deduce that the increase in lipidated mammalian Atg8 proteins in response to nutrient starvation is due to post-translational regulation of the processing enzymes. To test this hypothesis, cells were starved for 3 or 13 h, after which they were lysed and the lysates were tested for their ability to cleave GATE-16. In this assay, recombinant GATE-16, tagged at both termini (His_6-GATE-16-HA), is used so that cleaved GATE-16 can be detected by its faster mobility in SDS–PAGE. As shown in Figure 4C, incubation of GATE-16 in a lysate prepared from cells that were starved for a short period of 3 h resulted in a decrease of up to 40% in the cleavage activity as compared with control cells. Starvation of cells for longer periods of 13 h (during which the cells are still viable) resulted in further inhibition in cleavage activity. However, addition of 1 mM DTT to the lysates brought about recovery of the cleavage activity, suggesting that the inhibition of Atg4 was caused by oxidation of the protein. Consistently, treatment of cells with 1 mM H_2O_2 for 1 h before lysis resulted in strong inhibition of the cleavage activity of Atg4 as compared with control cells. Addition of DTT to the lysate restored most of the lost activity, confirming that the inhibition by oxidation is reversible. Notably, the protein levels of the GATE-16-specific protease, HsAtg4A, did not change under any of the tested conditions (Supplementary Figure 4A), supporting the idea that the regulation of Atg4 activity is post-translational. Specific anti-HsAtg4A antibodies were utilized to confirm that the cleavage activity shown in Figure 4C is mediated by HsAtg4A (for details see Supplementary Figure 4B),

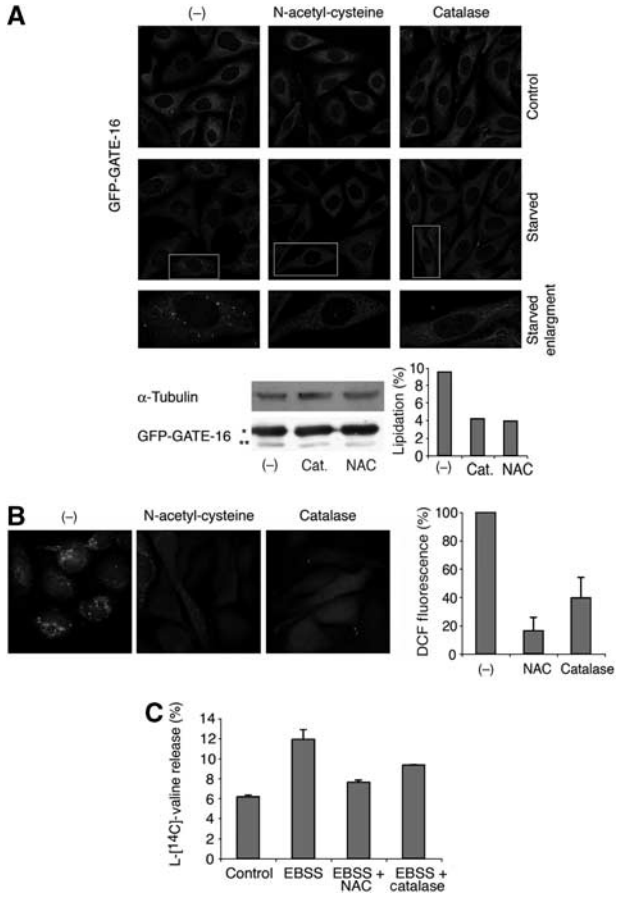

Figure 3 ROS accumulation is essential for autophagy. (**A**) Upper panel: CHO cells stably transfected with GFP-GATE-16 were pre-incubated in the presence or absence of 10 mM NAC or 1000 μ/ml catalase for 10 min before starvation for 2 h in the presence or absence of these drugs, or grown in a control medium containing the drugs for 2 h. The cells were then fixed, permeabilized and stained with anti-GFP monoclonal antibodies. Representative images are shown. Lower panel: HEK 293 cells were transfected with GFP-GATE-16. At 24 h post-transfection, the cells were treated with NAC or catalase and starved as explained above, lysed in Ripa buffer and 100 μg of each lysate was separated on 10% SDS–PAGE and subsequently analyzed with anti-GFP antibodies to detect the transfected GATE-16 and anti-tubulin antibodies as control. The data were quantified using NIH image program and are depicted as the percentage of lipidated protein from the total GATE-16. (*) indicates non-lipidated and (**) indicates lipidated GFP-GATE-16. (**B**) CHO cells treated with NAC or catalase and starved as detailed in (A) were incubated with DCFDA and visualized by a confocal microscope or analyzed by a fluorimeter as in Figure 1. (**C**) The rate of degradation of long-lived proteins was measured in CHO cells incubated in either α-MEM medium or EBSS medium, or following pretreatment with 10 mM NAC for 10 min or with 1000 μ/ml catalase overnight. A representative experiment is shown.

indicating that Atg4 is a target for redox regulation under starvation, and suggesting that accumulation of lipidated Atg8s under starvation might result from inhibition of Atg4 activity. Indeed, we found that treatment with 1 mM H_2O_2 resulted in accumulation of lipidated LC3 (Supplementary Figure 4C).

Atg4 acts both in the initial processing of Atg8s (priming) and in the delipidation step. The priming step was previously shown to occur immediately after translation under nutrient-rich conditions (Kabeya *et al*, 2000). To test whether this step is also inhibited during starvation, we transfected cells with GATE-16 tagged with Myc at its N-terminus and HA at the C-terminus, starved them for 30 min (a time period in which autophagosomes are expected to form; Fass *et al*, 2006) or 13 h and subjected them to a [^{35}S]methionine pulse–chase experiment as detailed in Materials and methods (Figure 4D). The control experiment shows that two bands at approximately 19 kDa are detected immediately after pulse labeling in the transfected cells (Figure 4D, left panel). A 1 h chase resulted in disappearance of the upper band, suggesting that this band corresponds to unprimed GATE-16 (Myc-GATE-16-HA), whereas the lower band corresponds to primed GATE-16 (Myc-GATE-16). Short starvation does not induce accumulation of the unprimed form (Figure 4D, middle panel), and this form accumulates only in cells that were starved for a long period of 13 h.

These results indicate that HsAtg4A is redox regulated during starvation. As the priming activity is not affected by short starvation, we conclude that the delipidation activity is the main target of this regulation.

To characterize the redox regulation of HsAtg4, we expressed HsAtg4A as a recombinant protein and tested its activity in the cell-free cleavage assay. As depicted in Figure 5A, the protease was gradually activated upon reduction of the reaction mixture and the activity saturated at 1 mM DTT. Next, we tested the inhibition of HsAtg4A activity by H_2O_2. The protein was preincubated in a low concentration of DTT for activation followed by addition of H_2O_2 for 5 min before incubation with GATE-16 for the cleavage assay. The activity of HsAtg4A decreased as the H_2O_2 concentration increased above 100 μM (Figure 5B). In some experiments, a slight increase in the protease activity was detected upon addition of 30 μM H_2O_2 to the reaction mixture. Finally, we tested the reversibility of HsAtg4 inhibition by H_2O_2. In this experiment, the protein was preincubated in a low concentration of DTT (Figure 5C, lane 2) followed by addition of H_2O_2 (lane 3) and then addition of a high concentration of DTT (lane 4; each incubated for 5 min before addition of the next reagent) before incubation with GATE-16. Under these conditions, HsAtg4A completely regained its activity. Taken together, these results show that reducing conditions activate HsAtg4A, whereas an oxidizing environment inhibits its activity. Moreover, these results indicate that H_2O_2 alone is sufficient to reversibly inhibit the activity of HsAtg4A *in vitro*, and therefore suggest that H_2O_2 might also act directly on the protease *in vivo*.

Cys^{81} is a target for the redox regulation of HsAtg4A

HsAtg4A contains 12 cysteines, seven of which are highly conserved among tetrapod homologues of Atg4A and Atg4B. The latter share an overall high conservation level with respect to the whole family (Figure 6). One of these conserved residues is the putative active residue of the protease Cys^{77} (Kirisako *et al*, 2000; Tanida *et al*, 2004a), the only cysteine conserved also in the yeast *S. cerevisiae* (Figure 6A, large arrow, numbering is according to HsAtg4B). Another conserved residue (Cys^{81} in HsAtg4A) is located four sites downstream of the active residue. We first sought to determine whether Cys^{77} is the catalytic residue, as suggested by homology to ScAtg4 and HsAtg4B. As shown in Figure 7A, recombinant HsAtg4A harboring a mutation of cysteine to alanine at position 77 (His_6-HsHsAtg4A^{C77A}) did not cleave

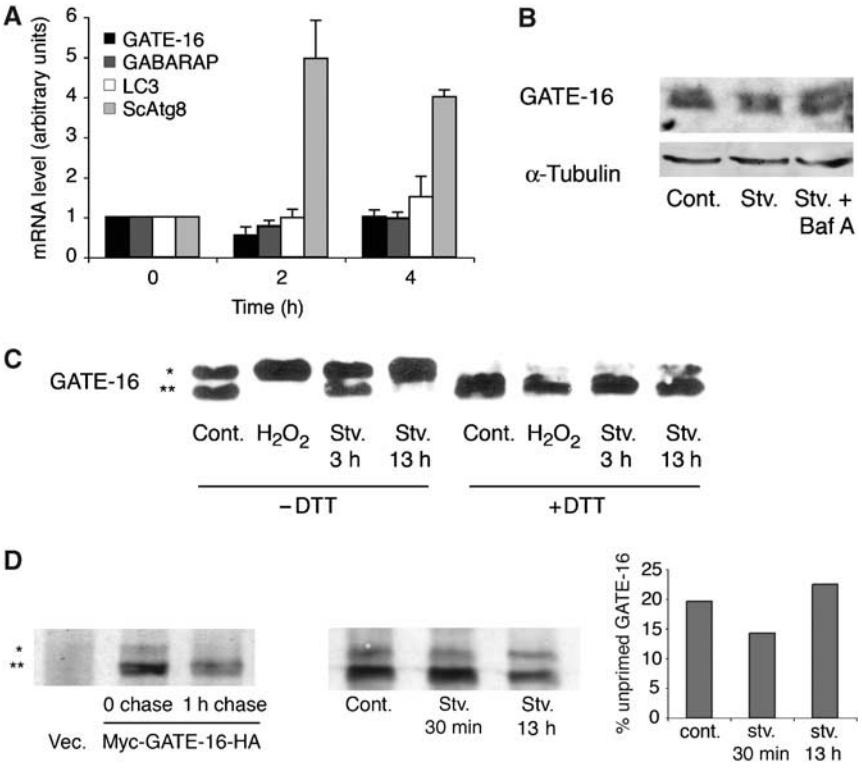

Figure 4 The activity of endogenous Atg4 is inhibited under nutrient starvation. (**A**) CHO cells (for mammalian Atg8s) or cells of *S. cerevisiae* (for ScAtg8) were incubated in starvation medium (EBSS or SD-N, respectively) for different time periods as indicated before isolation of RNA by the Tri-reagent as explained in Materials and methods. For each gene, data obtained from non-starved cells were set to an arbitrary value of 1, and results from the corresponding starved cells were normalized accordingly. Results represent the means ± s.d. of three separate experiments. (**B**) HEK 293 cells were grown in control medium or starved for 2 h in EBSS in the absence or presence of 100 nM bafilomycin A1. Lysates (100 μg) obtained in Ripa buffer were run on 12% SDS–PAGE and analyzed by Western blot, using anti-GATE-16 or anti-tubulin antibodies. (**C**) CHO cells were grown in a control medium in the presence or absence of 1 mM H_2O_2 for 1 h, or starved for 3 or 13 h. Lysates (10 μg) obtained in Ripa buffer were incubated with recombinant His_6-GATE-16-HA (0.3 μg) in 50 KT reaction buffer (25 mM Tris, pH 7.4, 50 mM KCl) at 30°C for 45 min, in the presence or absence of 1 mM DTT. The reaction was stopped by addition of sample buffer and boiling, after which the samples were resolved on 15% SDS–PAGE and subsequently analyzed by Western blot, using anti-His monoclonal antibodies. The experiment was repeated six times; a representative blot is shown. (**D**) Left panel: HeLa cells transfected with Myc-GATE-16-HA or with an empty vector as control were labeled with [^{35}S]methionine for 10 min and lysed immediately or chased for 1 h before lysis in Ripa buffer. Lysates were immunoprecipitated using anti-Myc antibodies and the immunoprecipitates were resolved on 15% SDS–PAGE. Middle panel: HeLa cells transfected with Myc-GATE-16-HA were kept in control medium or starved for 30 min or 13 h in EBSS before labeling with [^{35}S]methionine for 10 min, immediate lysis, analysis by SDS–PAGE and quantification (right panel) using NIH image program. Values are presented as the average percentage of unprimed form out of the total GATE-16. (*) in all sections of this figure indicates non-cleaved His_6-GATE-16-HA or Myc-GATE-16-HA and (**) indicates cleaved His_6-GATE-16 or Myc-GATE-16.

GATE-16 *in vitro*, neither in the absence nor in the presence of DTT. Based on this result and the sequence homology described above, we conclude that Cys^{77} is part of the active site of HsAtg4A.

To study the mechanism of redox regulation of HsAtg4A, we mutated the conserved cysteine residues 81 and 92 (Figure 6A, small arrows), which are closest to the active residue, to serine (His_6-$HsAtg4A^{C81S}$ and His_6-$HsAtg4A^{C92S}$, respectively) and tested their activity in the cell-free cleavage assay of GATE-16 under different redox conditions. As shown in Figure 7A, mutation in Cys^{81} significantly reduced the redox sensitivity of HsAtg4A so that His_6-$HsAtg4A^{C81S}$ was partially active even in the absence of DTT. Mutation in Cys^{92}, however, had no effect on the regulation and the protease remained under the same conditions as active as His_6-$HsAtg4A^{WT}$ (data not shown). Next, we tested the effect of oxidation by H_2O_2 on the activity of His_6-$HsAtg4A^{C81S}$. We found that the mutant protein retained significant activity in the presence of H_2O_2 (Figure 7B) under conditions in which the WT was completely inhibited (Figure 5C). Similar to the WT, the partial inhibition of His_6-$HsAtg4A^{C81S}$ by H_2O_2 could be reversed by addition of DTT. From these results, we conclude that Cys^{81} is important for redox regulation of HsAtg4A *in vitro*.

HsAtg4A and HsAtg4B are both redox regulated during autophagy

To examine whether Cys^{81} plays a role in the redox regulation of HsAtg4A *in vivo*, we monitored the formation of GFP-GATE-16-labeled autophagosomes in cells transfected with HsAtg4A mutants. Expression of $HsAtg4A^{C81S}$ significantly impaired the formation of GATE-16-labeled autophagosomes in starved cells (Figure 8A), as compared with cells expressing $HsAtg4A^{WT}$ (Figure 8A) or $HsAtg4A^{C92S}$ (data not shown) at similar levels. The average number of autophagosomes formed in $HsAtg4A^{C81S}$-expressing cells was 70% lower than in $HsAtg4A^{WT}$-expressing cells (Figure 8A, lower panel). One could suggest that in the presence of

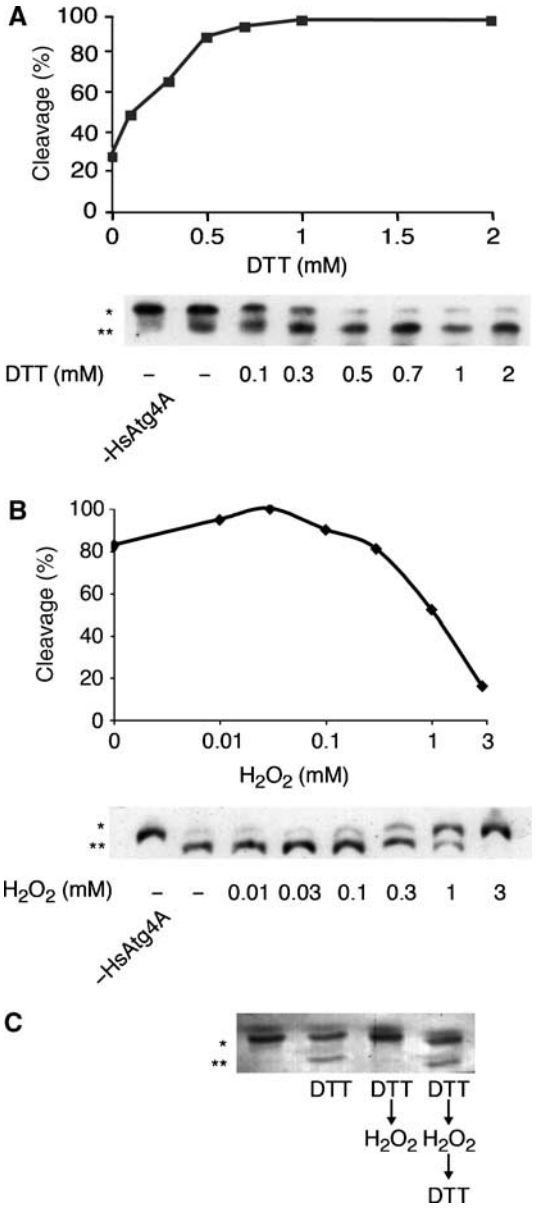

Figure 5 H_2O_2 directly inhibits the activity of HsAtgA. (**A**) Cleavage activity was tested by incubation of recombinant His_6-HsAtg4A (0.1 μg) and His_6-GATE-16-HA (0.3 μg) in 50 KT reaction buffer at 30°C for 45 min in the presence of indicated concentrations of DTT followed by Western blot analysis, using anti-His monoclonal antibodies. The resulting bands from three separate experiments were quantified with a densitometer using the Bio-Rad Multi-Analyst program and are presented as the average percentage of cleaved form out of the total GATE-16. (*) indicates non-cleaved His_6-GATE-16-HA and (**) indicates cleaved His_6-GATE-16. (**B**) His_6-HsAtg4A was incubated in the presence of 200 μM DTT at 4°C for 10 min. Reduced His_6-HsAtg4A (0.1 μg) was then incubated in 50 KT (to obtain 15 μM DTT) with the indicated concentrations of H_2O_2 at 25°C for 5 min, after which recombinant His_6-GATE-16-HA (0.3 μg) was added and incubation proceeded at 30°C for 45 min. Reaction mixtures from three separate experiments were analyzed and are presented as explained in (A). (**C**) His_6-HsAtg4A (0.1 μg) was incubated with recombinant His_6-GATE-16-HA (0.3 μg) after the following procedures: no treatment (lane 1); pretreatment with 200 μM DTT at 25°C for 5 min (lane 2); treatment with 200 μM DTT followed by treatment with 1 mM H_2O_2 at 25°C for 5 min (lane 3); and treatment with 200 μM DTT followed by treatment with 1 mM H_2O_2 for 5 min and then 2 mM DTT (lane 4). Reaction mixtures were analyzed by Western blot using anti-His monoclonal antibodies.

$HsAtg4A^{C81S}$, autophagosomes are formed, but then rapidly degraded, and therefore cannot be seen. To exclude this possibility, we inhibited the degradation of autophagosomes in the lysosome using bafilomycin A (Mousavi *et al*, 2001). This treatment did not affect the mutant phenotype, indicating that autophagosomes do not form in cells transfected with $HsAtg4A^{C81S}$ (data not shown). The finding that GATE-16-labeled autophagosomes do not form in $HsAtg4A^{C81S}$-expressing cells was further supported by GATE-16 lipidation measurements. As the $HsAtg4A^{C81S}$ mutant is less sensitive to oxidation, we expect the delipidation activity to be higher in starved cells transfected with this mutant as compared with cells transfected with $HsAtg4A^{WT}$. Indeed, we found nearly 40% less of the lipidated form of GATE-16 in cells transfected with $HsAtg4A^{C81S}$ as compared with cells transfected with $HsAtg4A^{WT}$ (Figure 8B). It should be mentioned that expression of $HsAtg4A^{C81S}$ did not affect the pattern of LC3 staining in the cells (data not shown), as expected, as HsAtg4A is specific for GATE-16 and does not process LC3. Taken together, our findings support the notion that Cys^{81} takes part in the redox regulation of HsAtg4A during autophagy.

In order to extend our study to other Atg4 family members, we decided to test the LC3-specific protease, HsAtg4B. To that end, we transfected cells with GFP-$HsAtg4B^{WT}$, GFP-$HsAtg4B^{C78S}$ or with GFP as control and tested the effect on lipidation of LC3 and formation of LC3-labeled autophagosomes. We found that overexpression of both GFP-$HsAtg4B^{WT}$ and GFP-$HsAtg4B^{C78S}$ reduced autophagosome formation and lipidation of LC3 (data not shown). This phenomenon was previously reported for overexpression of $HsAtg4B^{WT}$ (Tanida *et al*, 2004a). To overcome this problem, we added H_2O_2 to the starvation media. Under these conditions, $HsAtg4B^{WT}$ was inhibited and a normal autophagic phenotype was observed (Figure 9). $HsAtg4B^{C78S}$, however, was resistant to H_2O_2 and the cells expressing this construct failed to form lipidated LC3 and LC3-labeled autophagosomes. These results indicate that HsAtg4B, similar to HsAtg4A, is redox regulated.

Discussion

Autophagy is a unique pathway of intracellular trafficking activated in response to extracellular signals. Although many of the proteins involved in this process have been identified, the signal transduction pathway leading to activation of autophagy is not fully solved. Here we demonstrate, for the first time, the involvement of ROS as signaling molecules in starvation-induced autophagy. We show that starvation triggers accumulation of ROS, most probably H_2O_2, which is necessary for autophagosome formation and the resulting pathway of degradation. The oxidative signal is partially PI3K dependent, located upstream of the Atg5-dependent conjugation machinery. Furthermore, we identify a direct target for oxidation by H_2O_2—the protease Atg4.

Based on our results, we propose the following model, illustrated in Figure 10: nutrient starvation induces complex formation between class III PI3K and Beclin 1, which in turn leads, together with other signals, to a local rise in H_2O_2 in the vicinity of mitochondria. This oxidative signal leads to inactivation of Atg4 at the site of autophagosome formation, thereby promoting lipidation of Atg8, an essential step in the process of autophagy. As the autophagosome matures to-

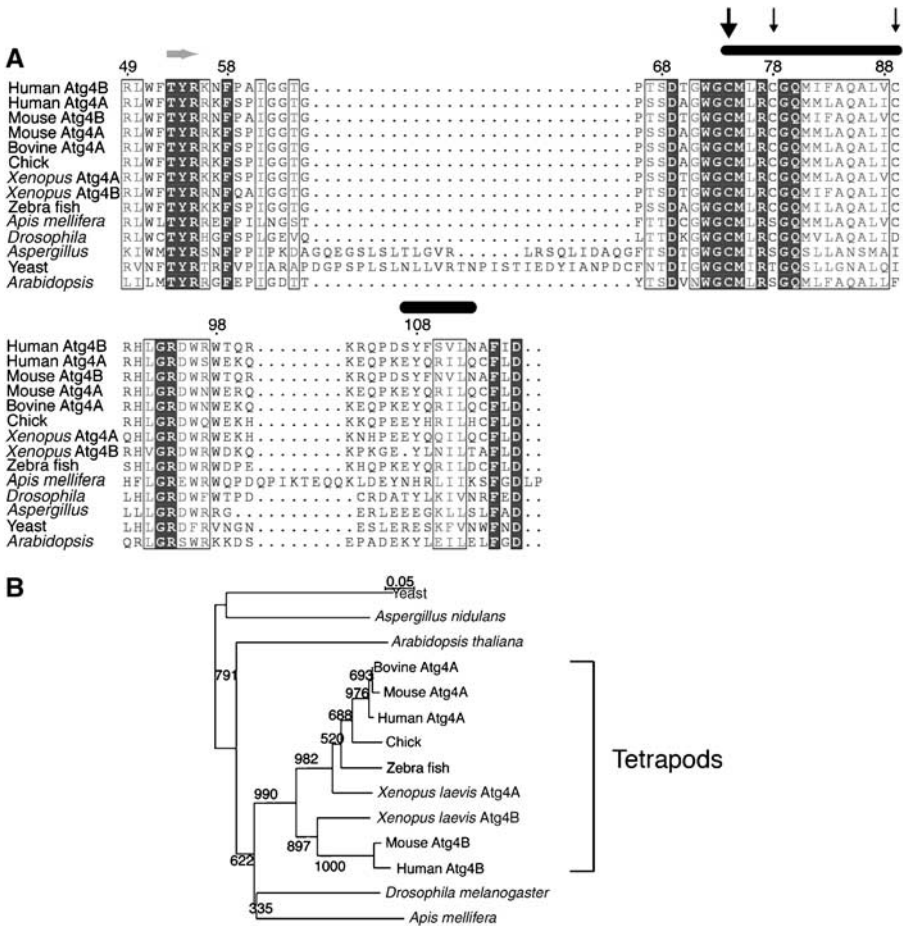

Figure 6 Tetrapod homologues of Atg4 share several conserved cysteine residues. (**A**) Amino-acid alignment of the region surrounding the active cysteine residue among members of the Atg4 family. Sequences of the following accession numbers are aligned: BAB83890, BAB83889, NP_777364, NP_777363, NP_001001171, CAG32326, AAH73017, AAH82660, AAH95617, XP_393739, NP_608563, XP_661074, NP_014176 and NP_191554. The alignment was preformed using the ClustalX multiple alignment program and is depicted by the ESPript 2.0 program, representing identity by a black frame and homology by a gray background. Numbering is according to the HsAtg4B sequence. α-Helices and a β-sheet found in this region according to the recently solved structure of HsAtg4B (Sugawara *et al*, 2005; Kumanomidou *et al*, 2006) are marked as black ellipses and a gray arrow, respectively. The catalytic cysteine residue is marked by a wide black arrow; other conserved cysteines are marked by thin black arrows. (**B**) A phylogenetic tree was created based on the alignment presented in (A) using the NJplot program (Perriere and Gouy, 1996). Bootstrap values indicating the reliability of the tree branches (with 1000 being the maximal value) are shown.

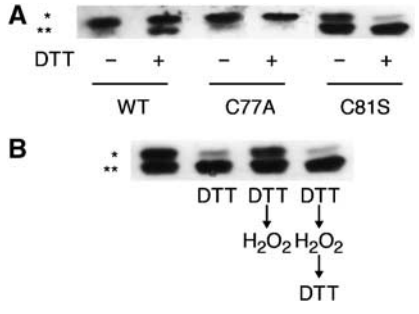

Figure 7 Mutation in Cys81 reduces the redox sensitivity of HsAtg4A *in vitro*. (**A**) Recombinant His_6-$HsAtg4A^{WT}$, His_6-$HsAtg4A^{C77A}$ or His_6-$HsAtg4A^{C81S}$ (0.1 μg) was incubated with His_6-GATE-16-HA (0.3 μg) in 50 KT reaction buffer at 30°C for 45 min in the presence or absence of 1 mM DTT. Reaction mixtures were analyzed by Western blot using anti-His monoclonal antibodies. (*) indicates non-cleaved His_6-GATE-16-HA and (**) indicates cleaved His_6-GATE-16. (**B**) His_6-$HsAtg4A^{C81S}$ (0.1 μg) was incubated with recombinant His_6-GATE-16-HA (0.3 μg) following the same procedure as detailed in Figure 5C. Reaction mixtures were analyzed and are presented as explained in (A).

wards fusion with the lysosome, its localization apparently changes to an H_2O_2-poor environment where Atg4 is active and can delipidate and recycle Atg8.

How does H_2O_2 regulate Atg4? Atg4s are cysteine proteases that share several conserved cysteine residues. One of these is the catalytic residue, found previously in other members of the Atg4 family and shown here to be Cys^{77} in HsAtg4A. Another conserved motif is a cysteine residue located four amino acids from the catalytic residue, Cys^{81} in HsAtg4A. Remarkably, we found this residue to be crucial for the redox regulation of HsAtg4A. Mutation of this residue to serine significantly impaired the sensitivity of the protein to H_2O_2 *in vitro*, and abolished the formation of GATE-16-labeled autophagosomes in cells. The essentiality of this residue for proper redox regulation was further confirmed by the finding that the corresponding HsAtg4B mutant ($HsAtg4B^{C78S}$) exhibited a similar autophagic defect. Our *in vitro* study shows that H_2O_2 directly inactivates Atg4. This could be accomplished either by binding of H_2O_2 to Cys^{77} or to Cys^{81}, forming reversible sulfenic acid that shields Cys^{77}, or by oxidation,

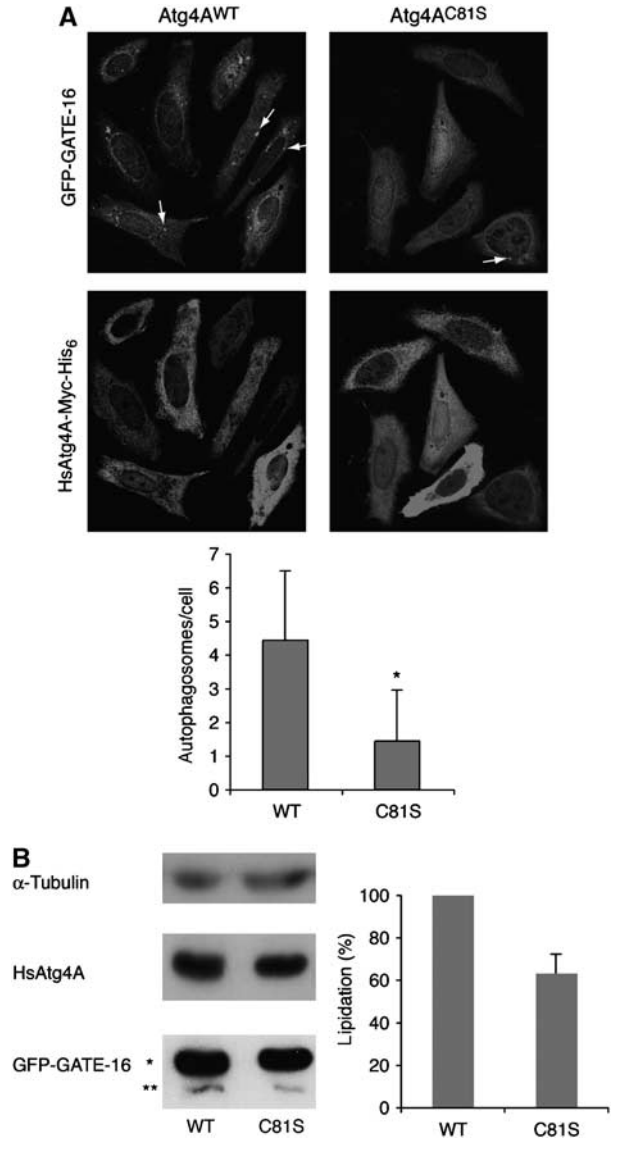

Figure 8 Cys 81 is required for redox regulation of HsAtg4A in cells. (**A**) CHO cells stably expressing GFP-GATE-16 were transiently transfected with HsAtg4A^{WT}-Myc-His$_6$ or HsAtg4A^{C81S}-Myc-His$_6$. At 24 h post-transfection, cells were starved for 2.5 h after which they were fixed, permeabilized and incubated with anti-Myc monoclonal antibodies. Upper panel: typical images of cells transfected with the above constructs, as visualized using a confocal microscope; representative autophagosomes are indicated by arrows. Lower panel: quantification of the average number of autophagosomes per cell in the different transfectants. Images of the fixed cells were visualized using a Nikon eclipse TE300 fluorescent microscope and used for quantification of the number of autophagosomes per cell. The results presented are the means ± s.d. of a total of 100 cells from three separate experiments. (*) indicates significance at $P<0.001$. (**B**) Left panel: HEK 293 cells were cotransfected with GFP-GATE-16 and each of the Atg4A constructs mentioned in (A). At 40 h post-transfection, the cells were starved for 2.5 h, lysed in Ripa buffer and 100 μg of each lysate was loaded to 10% SDS–PAGE and subsequently analyzed with anti-GFP antibodies to detect the transfected GATE-16, anti-Myc antibodies to detect the transfected HsAtg4A and anti-tubulin antibodies as control. (*) indicates non-lipidated GFP-GATE-16 and (**) indicates lipidated GFP-GATE-16. Right panel: results from three separate experiments, as detailed in the left panel, were analyzed using NIH image program and quantified as follows: the amount of lipidated GFP-GATE-16 out of the total of GFP-GATE-16 was calculated for each mutant in each experiment. The value obtained for HsAtg4A^{WT} in each experiment was set to 100% and the relative lipidation in cells transfected with the mutant was calculated accordingly.

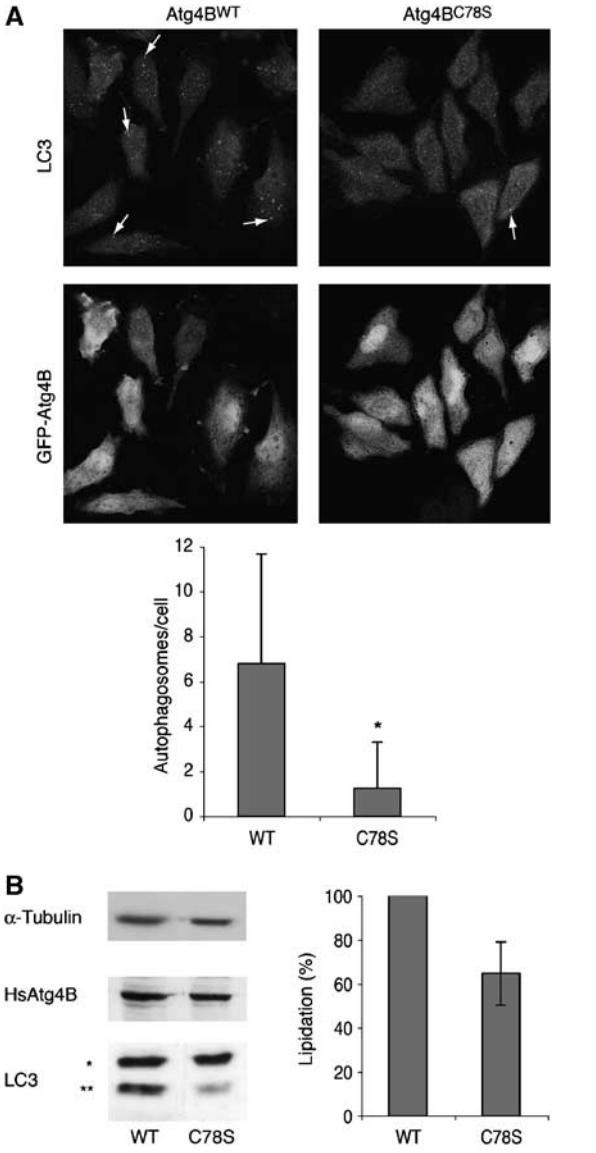

Figure 9 HsAtg4B is redox regulated during starvation in a similar mechanism to HsAtg4A. (**A**) HeLa cells were transiently transfected with GFP-HsAtg4B^{WT} or GFP-HsAtg4B^{C78S}. At 24 h post-transfection, cells were starved for 2.5 h in the presence of 4 mM H_2O_2 after which they were fixed, permeabilized and incubated with anti-LC3 polyclonal antibodies. Cells were visualized (upper panel) and quantified (lower panel) as explained in Figure 8. Representative autophagosomes are indicated in the upper panel by arrows. The results presented in the lower panel are the means ± s.d. of a total of 100 cells from three separate experiments. (*) indicates significance at $P<0.001$. (**B**) Left panel: HeLa cells transfected and treated as in (A) were lysed in Ripa buffer and 40 μg of each lysate was loaded to 12% SDS–PAGE and subsequently analyzed with anti-LC3 antibodies and anti-GFP antibodies to detect the transfected HsAtg4B and anti-tubulin antibodies as control. (*) indicates non-lipidated LC3 and (**) indicates lipidated LC3. Right panel: results from three separate experiments, as detailed in the left panel, were analyzed as explained in Figure 8B.

which leads to other modifications such as formation of a disulfide bond between Cys^{77} and Cys^{81}, again shielding Cys^{77}. Such a disulfide bond, however, was not detected in our experiments (unpublished data). Alternatively, H_2O_2 might be affecting a different site, which is altered when Cys^{81} is

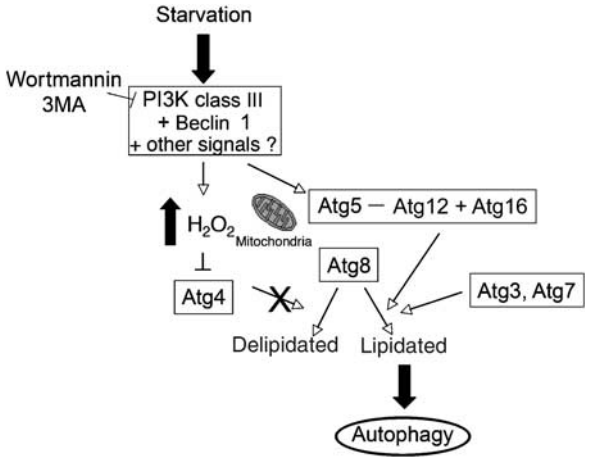

Figure 10 A proposed model for the redox regulation of autophagy.

mutated. The active site, Cys^{77}, is conserved from yeast to man, whereas Cys^{81} is conserved only in tetrapod homologues of Atg4A and Atg4B. Lower species harbor a conserved Ser or Thr in this residue and hence the choice of a C81S mutant. We thus propose that the redox regulation may be mediated via Cys^{77} in lower species, whereas tetrapods evolved a more complex mechanism of regulation that requires both Cys^{77} and Cys^{81}, where the latter provides tetrapods with higher sensitivity to ROS than lower species. The recently solved three-dimentional structure of HsAtg4B (Sugawara *et al*, 2005; Kumanomidou *et al*, 2006) supports our model, as it shows Cys^{77} and Cys^{81} to be situated at the beginning of an α-helix, both facing the same plane of the helix. With such close proximity between the two cysteines, modifications on Cys^{81} could indeed affect the active site. Notably, both crystals were prepared under reducing conditions, and consequently no disulfide bridges or other modifications were reported for any of the cysteine residues.

Cysteine-harboring proteins serve as redox sensors. They can undergo rapid, variable and, most importantly, reversible post-translational modifications in response to changes in the oxidative conditions of the environment (Sitia and Molteni, 2004). Several cysteine proteases, including cathepsin D, cathepsin B and the cytosolic caspase-3 (Chandler *et al*, 1998) and calpains (Glading *et al*, 2001), have been shown to undergo redox regulation through a direct modification of the active site (reviewed in Giles *et al*, 2003). Redox regulation of Atg4 can provide rapid activation and inactivation of this protease, as part of the signaling pathway, leading to induction of the autophagic process.

A growing body of evidence suggests that autophagy plays a dual role, both in survival and in death-related pathways (Cuervo, 2003; Codogno and Meijer, 2005; Reef *et al*, 2006). The data available till now, linking ROS with autophagy, describe the death-related pathway, known as type II PCD, which is induced by high levels of ROS (i.e. oxidative stress; Yu *et al*, 2004; Kiffin *et al*, 2006). Recently, it has been shown that caspase inhibition leading to cell death through autophagy involves accumulation of ROS, owing to catalase-specific autophagic degradation. In that study, however, starvation did not lead to a similar effect (Yu *et al*, 2006). In our system, the rise in ROS is both local and reversible; it is not deleterious to cells and serves to oxidize a specific target. Therefore, our study provides the first indication for the involvement of ROS in starvation-induced autophagy as signaling molecules in a survival pathway.

Materials and methods

All experiments presented in the Results section were repeated at least three times unless indicated otherwise.

Expression and purification of recombinant proteins

Recombinant His_6-HsAtg4A (WT and the mutants described in Supplementary data) and His_6-GATE-16-HA were expressed from the pQE-30 plasmid and purified as described previously (Scherz-Shouval *et al*, 2003). Purification of His_6-HsAtg4A (WT and mutants) was carried out in the presence of 10 mM βME to prevent formation of nonspecific disulfide bonds; however, before its use, the protein was diluted to at least 30-fold or dialyzed in a buffer lacking βME.

Cell culture, transfection, reagents and immunofluorescence

All cell lines were grown in α-MEM medium (Biological Industries, Israel) supplemented with 10% fetal calf serum and referred to as control medium. Atg5−/− MEFs and anti-Atg16 polyclonal antibodies were a kind gift from the laboratory of Dr Mizushima (The Tokyo Metropolitan Institute of Medical Science). Stable clones of GFP-GATE-16-, GFP-LC3- or YFP-Atg5-transfected CHO cells were selected in 1 mg/ml geneticin (G418). Starvation was carried out in EBSS. Details regarding the use of different reagents for tissue culture treatments are described in Supplementary data. Transfections of CHO cells were preformed with lipofectamine (Invitrogen) according to the manufacturer's protocol. Transfections of HeLa and HEK 293 cells were performed by the standard calcium phosphate technique. For immunofluoresence, unless described otherwise, cells were fixed in methanol, permeabilized with acetone and then incubated with the indicated antibodies and visualized by a Nikon eclipse TE300 fluorescent microscope or by an Olympus IX-70 confocal microscope.

Hydrogen peroxide measurements

H_2O_2 was measured using 50 μMDHE (Molecular Probes) and 30 μM DCFDA (Molecular Probes). See Supplementary data for details. The fluorescent signal was detected by an Olympus IX-70 confocal microscope. Each experiment was repeated at least three times and representative images are shown. The DCFDA signal was also measured by a SPECTRAmax gimini fluorimeter, set to 485 excitation and 535 emission and kept at 37°C, for 40 min. Data collected from the fluorometric measurements were analyzed as detailed in Supplementary data. The results presented for all fluorimetric measurements are the means ± s.d. of at least three experiments in duplicate or triplicate.

Protein degradation assay

The assay was preformed on CHO cells according to the protocol described by Fass *et al* (2006). When required, 10 mM 3MA, 100 nM wortmannin, 1000 μ/ml catalase or 10 mM NAC were added. Notably, NAC was added for 10 min before starvation induction and catalase was added 14 h before starvation. [^{14}C]valine release was calculated as a percentage of the radioactivity in the TCA-soluble supernatant relative to the total cell radioactivity.

Preparation of cell lysates

Cells were homogenized in Ripa buffer (0.1 M NaCl, 5 mM EDTA, 0.1 M Na_2HPO_4/NaH_2PO4, pH 7.5, 1% Triton, 0.5% DOC, 0.1% SDS and protease inhibitors) by vortexing on ice. The homogenates were centrifuged for 15 min at 20 000 *g* and the supernatant containing the lysate was collected.

mRNA measurement

RNA was isolated by Tri-reagent (Molecular Research Center Inc.) as detailed in Supplementary data.

Pulse–chase experiment

HeLa cells were transiently transfected with Myc-GATE-16-HA or with an empty vector. Cells were then kept in full medium for 24 h, after which they were either incubated in methionine-free medium for 10 min or starved in EBSS for 30 min (2 × 10 cm plates). For long starvation, the cells (three plates) were shifted to EBSS 10 h post-transfection for 13 h, after which the medium was replaced with fresh EBSS. All cells were then pulse-labeled with 0.2 mCi of [^{35}S]methionine for 10 min at 37°C, and either chased in full medium for 1 h at 37°C or lysed immediately on ice, in Ripa buffer supplemented with 0.5 mM *N*-ethylmaleimide (sigma). Lysates were immunoprecipitated with anti-Myc antibodies and analyzed on 15% SDS–PAGE.

Supplementary data

Supplementary data are available at *The EMBO Journal* Online (http://www.embojournal.org).

Acknowledgements

We thank Vladimir Kish for invaluable guidance with the confocal microscope and Frida Shimron for her devoted assistance. We also thank Avihai Danon for his insights. This work was supported in part by grants from the Israel Science Foundation, Binational Science Foundation and by the Minerva center.

References

Cathcart R, Schwiers E, Ames BN (1983) Detection of picomole levels of hydroperoxides using a fluorescent dichlorofluorescein assay. *Anal Biochem* **134:** 111–116

Chandler JM, Cohen GM, MacFarlane M (1998) Different subcellular distribution of caspase-3 and caspase-7 following Fas-induced apoptosis in mouse liver. *J Biol Chem* **273:** 10815–10818

Codogno P, Meijer AJ (2005) Autophagy and signaling: their role in cell survival and cell death. *Cell Death Differ* **12** (Suppl 2)**:** 1509–1518

Cuervo AM (2003) Autophagy and aging—when 'all you can eat' is yourself. *Sci Aging Knowledge Environ* **2003:** pe25

Cuervo AM (2004) Autophagy: in sickness and in health. *Trends Cell Biol* **14:** 70–77

Fass E, Shvets E, Degani I, Hirschberg K, Elazar Z (2006) Microtubules support production of starvation-induced autophagosomes but not their targeting and fusion with lysosomes. *J Biol Chem* **281:** 36303–36316

Giles NM, Watts AB, Giles GI, Fry FH, Littlechild JA, Jacob C (2003) Metal and redox modulation of cysteine protein function. *Chem Biol* **10:** 677–693

Glading A, Uberall F, Keyse SM, Lauffenburger DA, Wells A (2001) Membrane proximal ERK signaling is required for M-calpain activation downstream of epidermal growth factor receptor signaling. *J Biol Chem* **276:** 23341–23348

Hemelaar J, Lelyveld VS, Kessler BM, Ploegh HL (2003) A single protease, Apg4B, is specific for the autophagy-related ubiquitin-like proteins GATE-16, MAP1-LC3, GABARAP, and Apg8L. *J Biol Chem* **278:** 51841–51850

Huang WP, Klionsky DJ (2002) Autophagy in yeast: a review of the molecular machinery. *Cell Struct Funct* **27:** 409–420

Ichimura Y, Kirisako T, Takao T, Satomi Y, Shimonishi Y, Ishihara N, Mizushima N, Tanida I, Kominami E, Ohsumi M, Noda T, Ohsumi Y (2000) A ubiquitin-like system mediates protein lipidation. *Nature* **408:** 488–492

Jabs T (1999) Reactive oxygen intermediates as mediators of programmed cell death in plants and animals. *Biochem Pharmacol* **57:** 231–245

Kabeya Y, Mizushima N, Ueno T, Yamamoto A, Kirisako T, Noda T, Kominami E, Ohsumi Y, Yoshimori T (2000) LC3, a mammalian homologue of yeast Apg8p, is localized in autophagosome membranes after processing. *EMBO J* **19:** 5720–5728

Kabeya Y, Mizushima N, Yamamoto A, Oshitani-Okamoto S, Ohsumi Y, Yoshimori T (2004) LC3, GABARAP and GATE16 localize to autophagosomal membrane depending on form-II formation. *J Cell Sci* **117:** 2805–2812

Kiffin R, Bandyopadhyay U, Cuervo AM (2006) Oxidative stress and autophagy. *Antioxid Redox Signal* **8:** 152–162

Kirisako T, Baba M, Ishihara N, Miyazawa K, Ohsumi M, Yoshimori T, Noda T, Ohsumi Y (1999) Formation process of autophagosome is traced with Apg8/Aut7p in yeast. *J Cell Biol* **147:** 435–446

Kirisako T, Ichimura Y, Okada H, Kabeya Y, Mizushima N, Yoshimori T, Ohsumi M, Takao T, Noda T, Ohsumi Y (2000) The reversible modification regulates the membrane-binding state of Apg8/Aut7 essential for autophagy and the cytoplasm to vacuole targeting pathway. *J Cell Biol* **151:** 263–276

Kissova I, Deffieu M, Samokhvalov V, Velours G, Bessoule JJ, Manon S, Camougrand N (2006) Lipid oxidation and autophagy in yeast. *Free Radic Biol Med* **41:** 1655–1661

Klionsky DJ, Cregg JM, Dunn Jr WA, Emr SD, Sakai Y, Sandoval IV, Sibirny A, Subramani S, Thumm M, Veenhuis M, Ohsumi Y (2003) A unified nomenclature for yeast autophagy-related genes. *Dev Cell* **5:** 539–545

Kumanomidou T, Mizushima T, Komatsu M, Suzuki A, Tanida I, Sou YS, Ueno T, Kominami E, Tanaka K, Yamane T (2006) The crystal structure of human Atg4b, a processing and de-conjugating enzyme for autophagosome-forming modifiers. *J Mol Biol* **355:** 612–618

Lang T, Schaeffeler E, Bernreuther D, Bredschneider M, Wolf DH, Thumm M (1998) Aut2p and Aut7p, two novel microtubule-associated proteins are essential for delivery of autophagic vesicles to the vacuole. *EMBO J* **17:** 3597–3607

Lee YJ, Cho HN, Soh JW, Jhon GJ, Cho CK, Chung HY, Bae S, Lee SJ, Lee YS (2003) Oxidative stress-induced apoptosis is mediated by ERK1/2 phosphorylation. *Exp Cell Res* **291:** 251–266

Macip S, Igarashi M, Berggren P, Yu J, Lee SW, Aaronson SA (2003) Influence of induced reactive oxygen species in p53-mediated cell fate decisions. *Mol Cell Biol* **23:** 8576–8585

Mann SS, Hammarback JA (1994) Molecular characterization of light chain 3. A microtubule binding subunit of MAP1A and MAP1B. *J Biol Chem* **269:** 11492–11497

Marino G, Uria JA, Puente XS, Quesada V, Bordallo J, Lopez-Otin C (2003) Human autophagins, a family of cysteine proteinases potentially implicated in cell degradation by autophagy. *J Biol Chem* **278:** 3671–3678

Mizushima N, Kuma A, Kobayashi Y, Yamamoto A, Matsubae M, Takao T, Natsume T, Ohsumi Y, Yoshimori T (2003) Mouse Apg16L, a novel WD-repeat protein, targets to the autophagic isolation membrane with the Apg12–Apg5 conjugate. *J Cell Sci* **116:** 1679–1688

Mizushima N, Yamamoto A, Hatano M, Kobayashi Y, Kabeya Y, Suzuki K, Tokuhisa T, Ohsumi Y, Yoshimori T (2001) Dissection of autophagosome formation using Apg5-deficient mouse embryonic stem cells. *J Cell Biol* **152:** 657–668

Mousavi SA, Kjeken R, Berg TO, Seglen PO, Berg T, Brech A (2001) Effects of inhibitors of the vacuolar proton pump on hepatic heterophagy and autophagy. *Biochim Biophys Acta* **1510:** 243–257

Ohsumi Y (2001) Molecular dissection of autophagy: two ubiquitin-like systems. *Nat Rev Mol Cell Biol* **2:** 211–216

Perriere G, Gouy M (1996) WWW-query: an on-line retrieval system for biological sequence banks. *Biochimie* **78:** 364–369

Petiot A, Ogier-Denis E, Blommaart EF, Meijer AJ, Codogno P (2000) Distinct classes of phosphatidylinositol 3′-kinases are involved in signaling pathways that control macroautophagy in HT-29 cells. *J Biol Chem* **275:** 992–998

Preston TJ, Muller WJ, Singh G (2001) Scavenging of extracellular H_2O_2 by catalase inhibits the proliferation of HER-2/Neu-transformed rat-1 fibroblasts through the induction of a stress response. *J Biol Chem* **276:** 9558–9564

Reef S, Zalckvar E, Shifman O, Bialik S, Sabanay H, Oren M, Kimchi A (2006) A short mitochondrial form of p19ARF induces autophagy and caspase-independent cell death. *Mol Cell* **22:** 463–475

Sagiv Y, Legesse-Miller A, Porat A, Elazar Z (2000) GATE-16, a membrane transport modulator, interacts with NSF and the Golgi v-SNARE GOS-28. *EMBO J* **19:** 1494–1504

Sakurai K, Cederbaum AI (1998) Oxidative stress and cytotoxicity induced by ferric-nitrilotriacetate in HepG2 cells that express cytochrome *P*450 2E1. *Mol Pharmacol* **54:** 1024–1035

Scherz-Shouval R, Sagiv Y, Shorer H, Elazar Z (2003) The COOH terminus of GATE-16, an intra-Golgi transport modulator, is

cleaved by the human cysteine protease HsApg4A. *J Biol Chem* **278:** 14053–14058

Shintani T, Klionsky DJ (2004) Autophagy in health and disease: a double-edged sword. *Science* **306:** 990–995

Sitia R, Molteni SN (2004) Stress, protein (mis)folding, and signaling: the redox connection. *Sci STKE* **2004:** pe27

Sugawara K, Suzuki NN, Fujioka Y, Mizushima N, Ohsumi Y, Inagaki F (2005) Structural basis for the specificity and catalysis of human Atg4B responsible for mammalian autophagy. *J Biol Chem* **280:** 40058–40065

Suzuki K, Kirisako T, Kamada Y, Mizushima N, Noda T, Ohsumi Y (2001) The pre-autophagosomal structure organized by concerted functions of APG genes is essential for autophagosome formation. *EMBO J* **20:** 5971–5981

Tanida I, Sou YS, Ezaki J, Minematsu-Ikeguchi N, Ueno T, Kominami E (2004a) HsAtg4B/HsApg4B/autophagin-1 cleaves the carboxyl termini of three human Atg8 homologues and delipidates microtubule-associated protein light chain 3- and GABAA receptor-associated protein-phospholipid conjugates. *J Biol Chem* **279:** 36268–36276

Tanida I, Ueno T, Kominami E (2004b) LC3 conjugation system in mammalian autophagy. *Int J Biochem Cell Biol* **36:** 2503–2518

Tassa A, Roux MP, Attaix D, Bechet DM (2003) Class III phosphoinositide 3-kinase–Beclin1 complex mediates the amino acid-dependent regulation of autophagy in C2C12 myotubes. *Biochem J* **376:** 577–586

Vanden Hoek TL, Li C, Shao Z, Schumacker PT, Becker LB (1997) Significant levels of oxidants are generated by isolated cardiomyocytes during ischemia prior to reperfusion. *J Mol Cell Cardiol* **29:** 2571–2583

Wang H, Bedford FK, Brandon NJ, Moss SJ, Olsen RW (1999) GABA(A)-receptor-associated protein links GABA(A) receptors and the cytoskeleton. *Nature* **397:** 69–72

Xu J, Yu S, Sun AY, Sun GY (2003) Oxidant-mediated AA release from astrocytes involves cPLA(2) and iPLA(2). *Free Radic Biol Med* **34:** 1531–1543

Yu L, Alva A, Su H, Dutt P, Freundt E, Welsh S, Baehrecke EH, Lenardo MJ (2004) Regulation of an ATG7-beclin 1 program of autophagic cell death by caspase-8. *Science* **304:** 1500–1502

Yu L, Wan F, Dutta S, Welsh S, Liu Z, Freundt E, Baehrecke EH, Lenardo M (2006) Autophagic programmed cell death by selective catalase degradation. *Proc Natl Acad Sci USA* **103:** 4952–4957

